SUMMARY REPORT

NASA GRANT (NAG 1-1652)

DEVELOPMENT OF ANALYSIS METHODS FOR DESIGNING WITH COMPOSITES

SUBMITTED TO

LaRC Grant Officer
Mail Stop 126
100 NASA Road
Hampton, VA 23681-2199

SUBMITTED BY

E. Madenci

Department of Aerospace and Mechanical Engineering
The University of Arizona
Tucson, AZ 85721

July 1999

NASA GRANT (NAG 1-1652)

DEVELOPMENT OF ANALYSIS METHODS FOR DESIGNING WITH COMPOSITES

This project involved the development of new analysis methods to achieve efficient design of composite structures. Specifically, it focused on five different analysis methods:

1) Stability and stress analysis of flat laminates with a cutout under general in-plane loading.

2) A new stiffened shell finite element in modeling built-up structures.

3) Pre- and post-processors for buckling analysis programs developed at NASA LaRC.

4) Optimum bolt spacing of single-lap joints by a Genetic Algorithm.

5) Probabilistic and deterministic approach for assessment of multi-site damage.

Under this grant, we accomplished the following, specific to each of these tasks.

Stability and Stress Analysis of Flat Laminates with a Cutout

We developed a complex variational formulation to analyze the in-plane and bending coupling response of an unsymmetrically laminated plate with an elliptical cutout subjected to arbitrary edge loading as shown in Figure 1. This formulation utilizes four independent complex potentials that satisfy the coupled in-plane and bending equilibrium equations, thus eliminating the area integrals from the strain energy expression. The solution to a finite geometry laminate under arbitrary loading is obtained by minimizing the total potential energy function and solving for the unknown coefficients of the complex potentials. The validity of this approach is demonstrated by comparison with finite element analysis predictions for a laminate with an inclined elliptical cutout under bi-axial loading.The geometry and loading of this laminate with a lay-up of [-45/45] are shown in Figure 2. The deformed configuration shown in Figure 3 reflects the presence of bending-stretching coupling. The validity of the present method is established by comparing the out-of-plane deflections along the boundary of the elliptical cutout from the present approach with those of the finite element method. The comparison shown in Figure 4 indicates remarkable agreement. The details of this method are described in a manuscript by Madenci et al. (1998).

This solution method is currently being extended to obtain the buckling response of symmetric flat laminates with cutouts subjected to in-plane edge loading. In order to permit general boundary conditions, constraint conditions in the form of Lagrange multipliers are introduced into the formulation. By applying this new solution method, we will investigate the influence of loading, boundary conditions, various cutout orientations, and lamination configurations on the buckling response of composite panels.

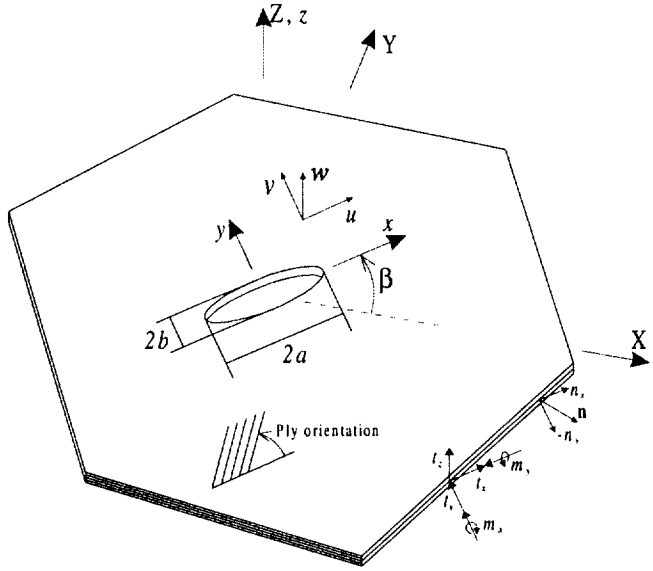

Figure 1. Finite geometry of a non-symmetric laminate with an inclined elliptical cutout.

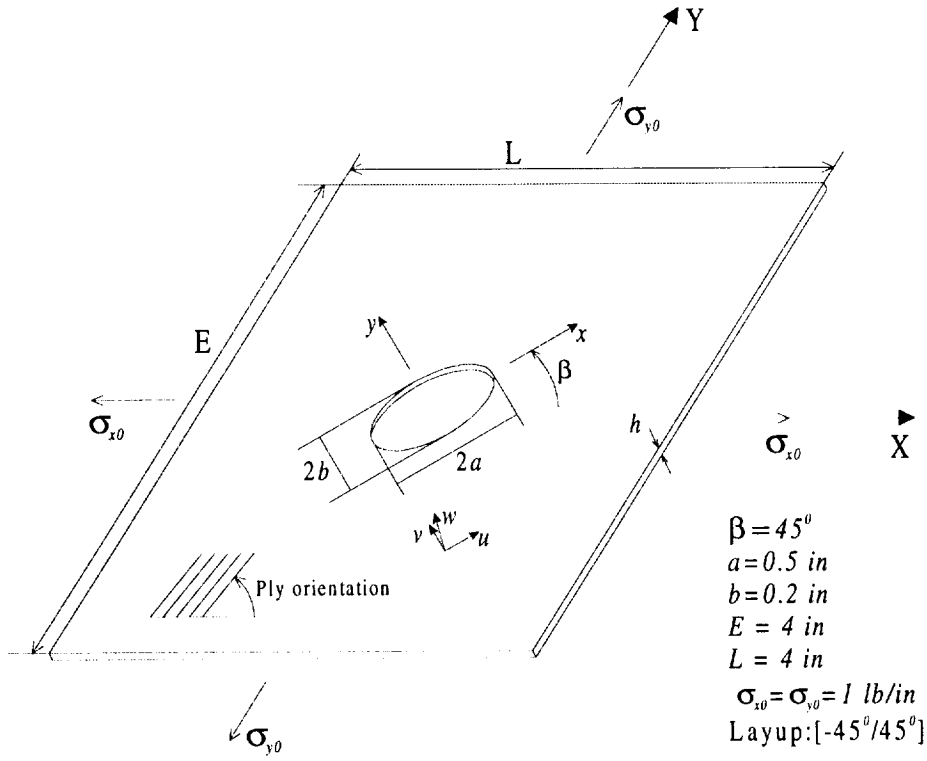

Figure 2. Square plate with an inclined elliptical cutout subjected to bi-axial tension.

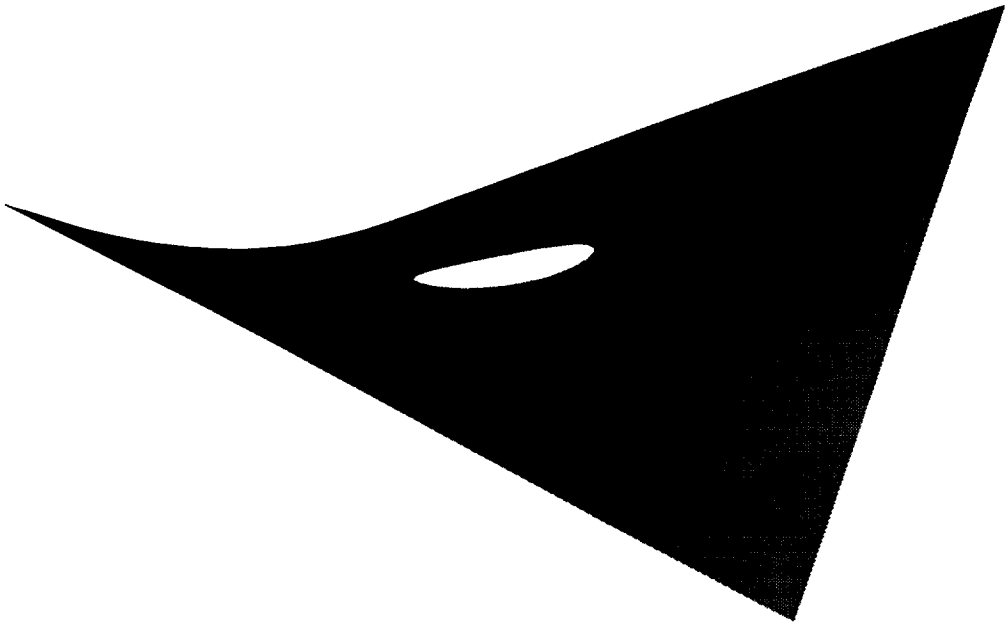

Figure 3. Deformed geometry of a square laminate with a 45° elliptical cutout.

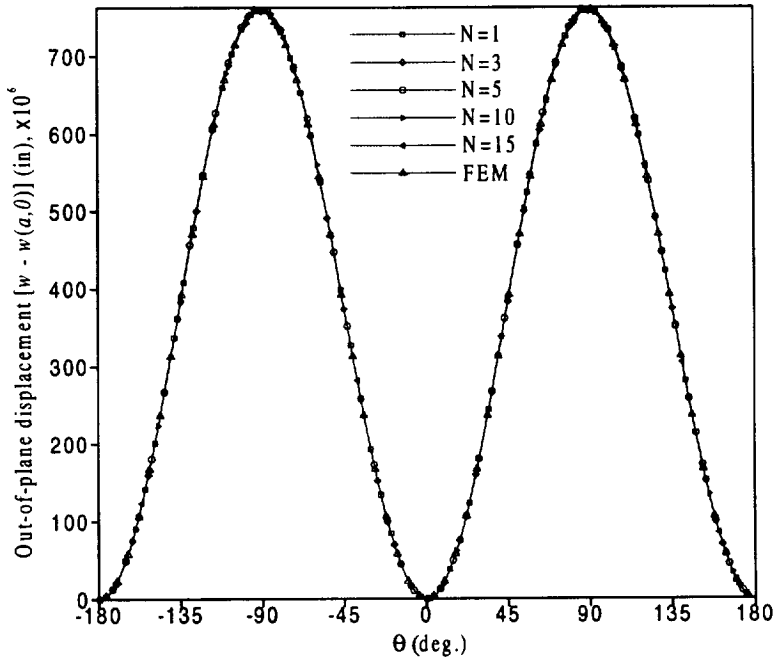

Figure 4. Comparison of out-of-plane displacements around the elliptical cutout.

A New Stiffened Shell Finite Element for Built-Up Structures

As an alternative to the conventional use of beam, plate, and shell elements to model the components of a stiffened shell separately, a new finite element that combines the kinematics of both the shell and stiffener in a single element has been developed. In this approach, stiffeners are integrated into the shell elements prior to the generation of the stiffness matrix. This is achieved by applying constraint of displacement continuity along the interface between the stiffener and the shell. These elements have proved to offer accuracy equal to the conventional elements and, most of all, practical use in many applications since the locations of stiffeners can be changed while keeping the mesh of the shell surface intact. The latter capability is expected to be extremely useful and reliable in the optimization of stiffened shell structures.

Both the shell and the beam (stiffener) elements account for transverse shear deformations and material anisotropy. The cross-section of the stiffener (beam) can be arbitrary in geometry and lamination. In order to combine the stiffener with the shell element, constraint conditions are applied to their displacement and rotation fields. These constraint conditions ensure that the cross-section of the stiffener remains co-planar with the section of the shell after deformation. While treating the shell nodal degrees of freedom as the only unknowns of this combined stiffened-shell element, the beam kinematics field is expressed in terms of the kinematics of the shell element through the constraint conditions. Therefore, not only are the total number of degrees of freedom reduced, but the discretization problems arising from the presence of stiffeners in conventional finite element applications are eliminated by letting the shell nodal degrees of freedom control the entire discretization. This stiffened shell element can be used in the discretization of unstiffened and stiffened shells containing multiple stiffeners without requiring constraint conditions to be applied in the structural level, as applied in conventional finite element discretizations. While specifying stiffeners within the shell elements, the discretization of the entire stiffened shell structure requires the presence of shell nodal points only. The complexity of the domain discretization caused by the presence of stiffeners is automatically avoided, and the additional degrees of freedom arising from the presence of stiffeners are eliminated, thereby reducing the total number of degrees of freedom. The geometry of the stiffened shell with a closer view of its section around the stiffener is shown in Figure 5. The nodal degrees of freedom associated with this element are shown in Figure 6.

This stiffened shell element has been validated against numerous benchmark solutions. The first problem is a curved cantilever stiffened plate with five equally spaced stiffeners and subjected to a vertical point load as shown in Figure 7a. The inner and outer radii of the curved (circular) plate are 4.5m and 5.5m, respectively. The plate and the stiffeners are both isotropic with Young's modulus 2.07×10^{11} kN/m^2 and Poisson's ratio 0.3. While one end of the plate is clamped, the other end is subjected to a vertical point load at the inner.

As depicted in Figure 7b, four different finite element discretizations, of orders (1×30), (2×20), (4×30), and (5×30), are considered in the analysis. This problem was previously studied by Jiang and Chernuka (1995). In their study, they presented a degenerated isoparametric stiffened shell element with 8 nodes. The results obtained from the present analysis and those reported by Jiang and Chernuka are shown in Figure 8a. The results converge to the actual solution as the grid size is increased. It is observed that the results from the present finite element model and those reported by Jiang and Chernuka using a (2×16) grid order are in close agreement.

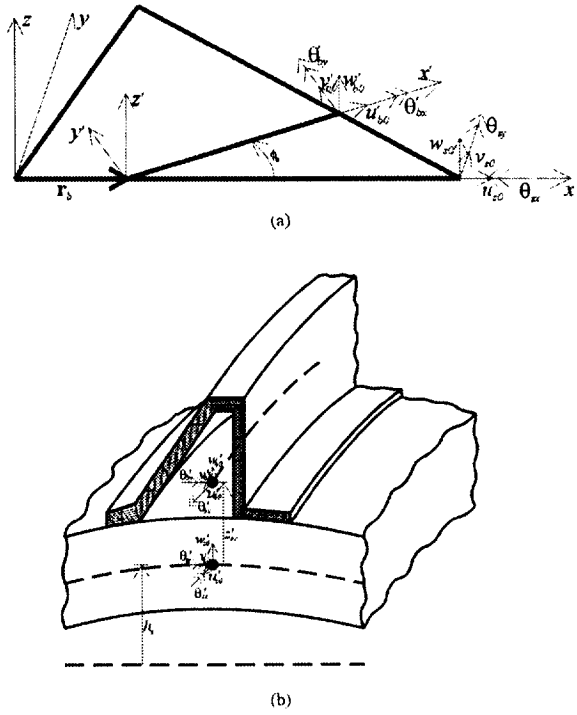

Figure 5. The geometric description of the stiffened shell element.

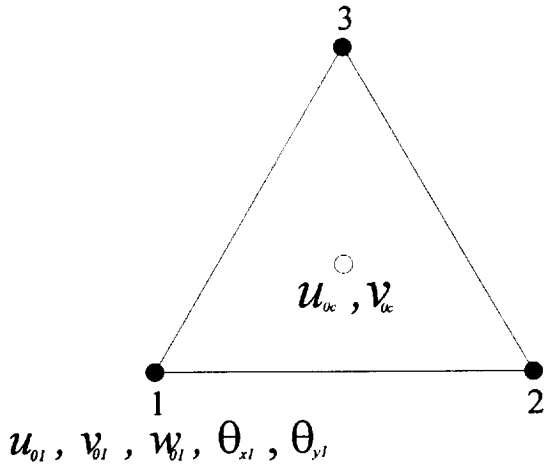

Figure 6. Nodal configuration for the degrees of freedom of the element.

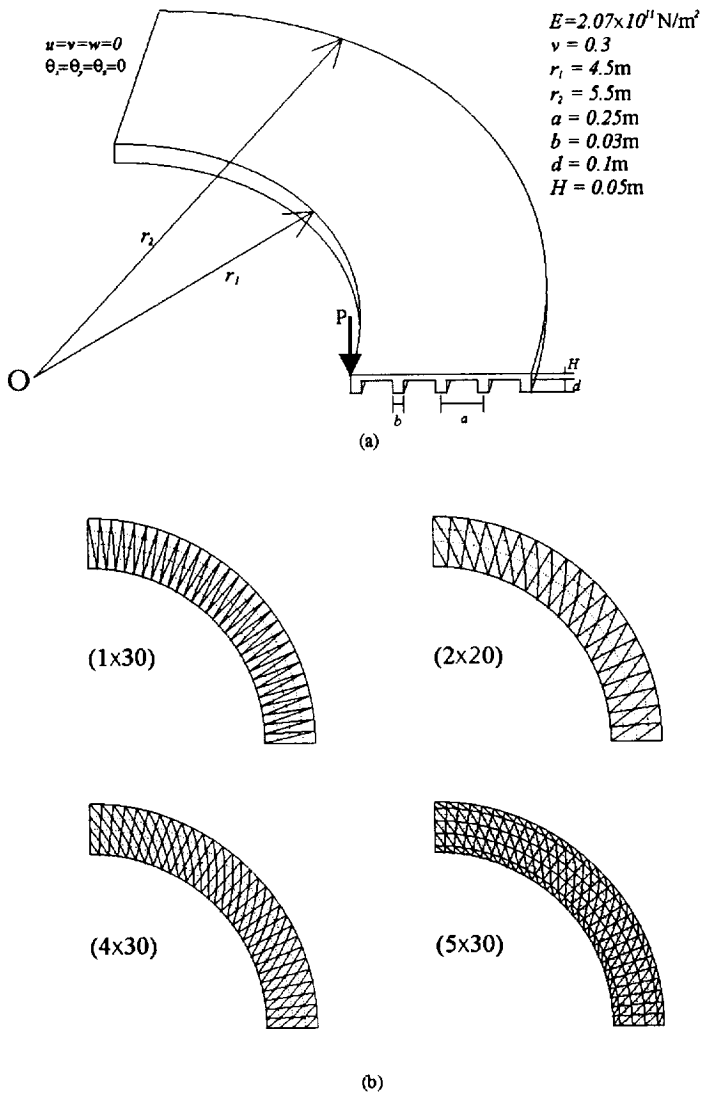

Figure 7. A curved cantilever stiffened plate subjected to a point load at one corner: (a) geometry and material description and (b) mesh discretization.

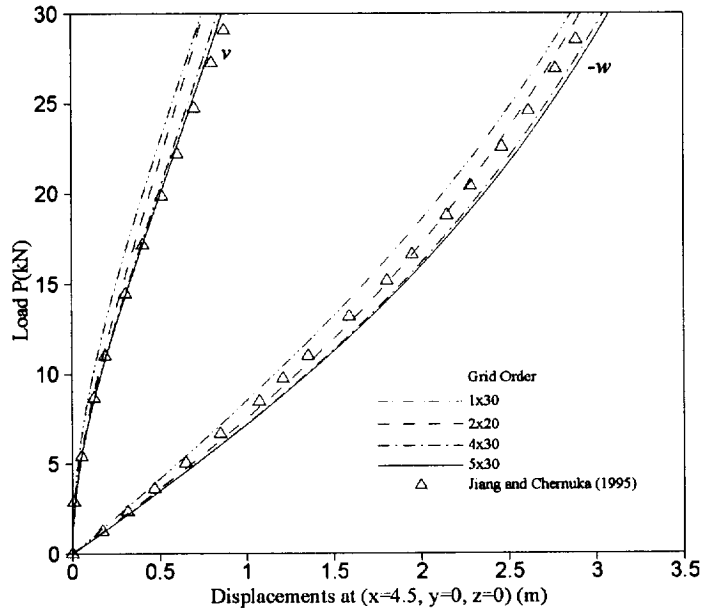

(a)

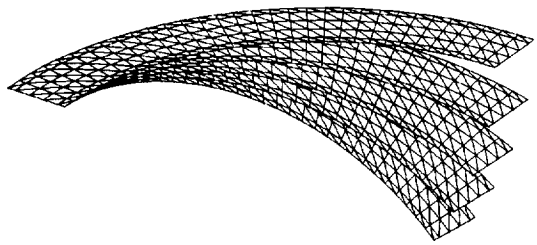

3-D view

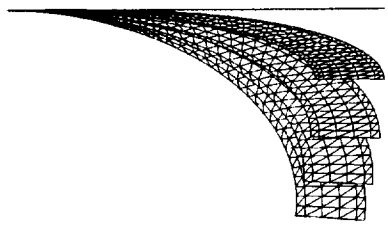

Front view

(b)

Figure 8. A curved cantilever stiffened plate subjected to a point load at one corner: (a) results and (b) sequence of deformed configurations.

The behavior of this stiffened shell is highly nonlinear in bending and twisting. As observed from the sequence of deformations depicted in Figure 8b, the present stiffened shell element can capture out-of-plane deflections of magnitude close to the radius of the curved plate. This figure shows that the maximum deflection occurs at the unloaded free corner of the plate. This is basically due to the bending deformations, which produce a slope higher than the twisting in the opposite direction at the free end of the curved plate.

The second validation problem involves a simply supported composite stiffened shell subjected to a uniform inward pressure as shown in Figure 9. The shell has the geometry of a spherical patch with radius R = 1000 inches. From the top view, the spherical patch has a square boundary with an edge length, $2a$, of 100 inches. The shell is made up of a cross-ply laminate having two layers with material properties $E_1 = 25\times10^6$psi, $E_2=10^6$psi, $G_{12}=0.5\times10^6$psi, $\nu_{12}=0.15$, and a ply thickness, t_k, equal to 0.5 inch. The cross-ply stacking sequence of the shell is [0°/90°/0°] from bottom to top. As shown in Figure 9a, the stiffeners are located along the two centerlines of the shell. The stiffeners also have cross-ply lay-up with four layers. The stacking sequence of these layers, from bottom to top, is $[0°/90°]_2$. The material properties are the same as those assigned for the shell, including the ply thickness. The stiffener width is specified as 2 inches.

In order to investigate the influence of stiffener eccentricity on the overall behavior of the stiffened shell, the unstiffened shell and three other stiffened cases, as shown in Figure 9b, having stiffeners on the bottom face of the shell, stiffeners on both faces of the shell (concentric), and stiffeners located on the top of the shell were studied. The cases with unstiffened and concentrically stiffened shells were also investigated by Liao and Reddy (1989). In their study, they used degenerated isoparametric shell and beam elements to discretize the patch. For this problem, the entire stiffened shell is modeled by 160 unstiffened and 36 stiffened shell elements as illustrated in Figure 10a, where the stiffeners are located along the cross-shaped patch of triangular elements.

This problem demonstrates the capability of the present stiffened shell element to capture the snap-through buckling behavior of the stiffened shell structure. Due to symmetry along the two centerlines, Liao and Reddy (1989) introduced symmetry conditions in order to model only one quarter of the stiffened shell. In the present finite element model, the symmetric buckling mode is captured by suppressing the horizontal displacements and rotations about the horizontal axes at the center of the stiffened shell. The results for all four cases are illustrated in Figure 10b. Also shown in this figure are the results obtained by Liao and Reddy, denoted by hollow triangular symbols. The comparisons between the present analysis and the analysis reported by Liao and Reddy are in close agreement for both unstiffened and concentrically stiffened cases. As observed from Figure 10b for all cases, the load carrying capacity of the stiffened shell against buckling is influenced by eccentricity of the stiffeners with respect to the shell middle surface. In this analysis, the snap-through buckling load increases as the stiffeners are gradually shifted from bottom to top. Furthermore, as expected, the presence of stiffeners increases the load carrying capacity compared to the unstiffened shell case. The details of this stiffened shell finite element are described in a manuscript by Barut et al. (1998).

Pre- and Post-Processors for Buckling Analysis Programs

We developed and demonstrated pre- and post-processors for the buckling analysis algorithm developed by Dr. M. Nemeth of NASA LaRC. Pre-processing prepares the input file for the solution algorithm and provides an on-screen sketch of the specific panel by defining (a) panel geometry, (b) laminate properties, and (c) loading and boundary conditions. Post-processing for analyzing the buckling response for specific parameters in the form of line plots is available. On-screen post-processing commands are mouse driven and/or use a drop-down menu. Printing from the screen or file is available through the post-processor. Figures 11-13 illustrate the pre- and post-processing capabilities of this design tool.

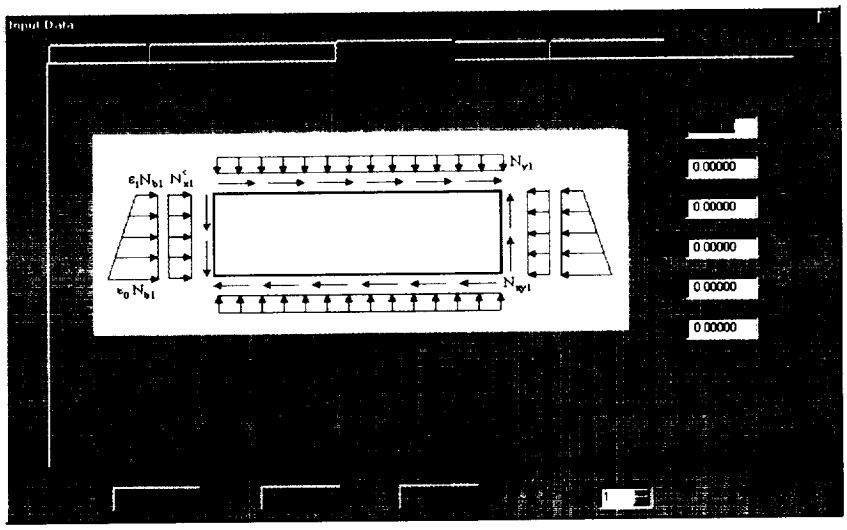

Figure 11. Input for the loading parameters.

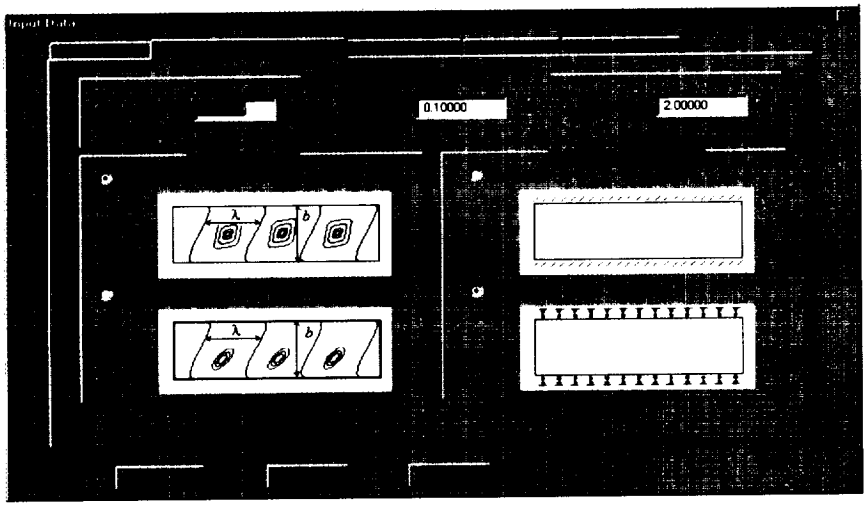

Figure 12. Imposition of the boundary conditions.

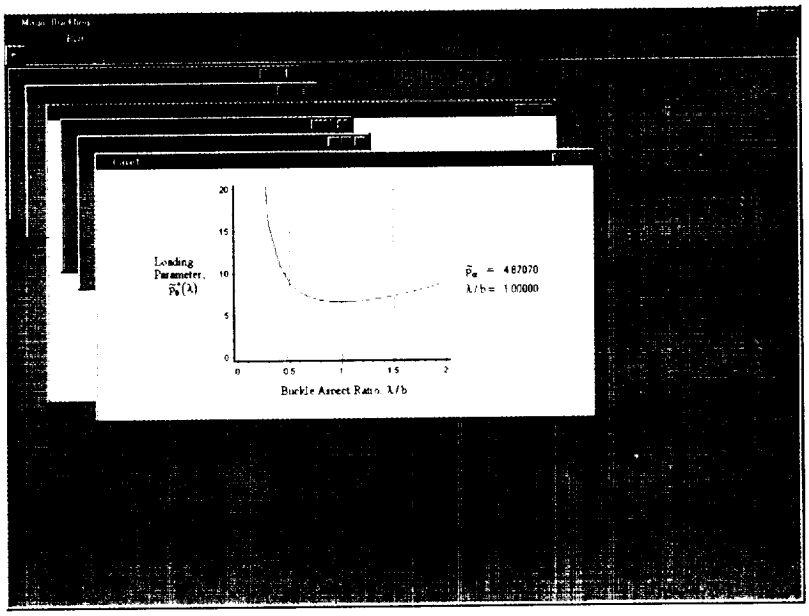

Figure 13. Typical display of results.

Optimum Bolt Spacing by a Genetic Algorithm

We demonstrated the application of the Genetic Algorithm (GA) to achieve an optimal single-lap bolted joint design with composite laminates. Although not a limitation, bolt spacing, bolt diameter, and degree of material anisotropy are considered as the primary design variables based on a previous study by Sergeev et al. (1998). The contact stresses (bolt loads) are determined by using a boundary collocation method. The bolt load distribution and the contact stresses, as well as the contact region, are determined as part of a non-linear solution. The solution method accounts for the effects of finite geometry and by-pass loading. Failure mode and load are predicted by employing the Maximum Strain Criterion, thus an evaluation function is established based this criterion. Two single-lap joint configurations with multiple fasteners, shown in Figures 14 and 15, are considered in order to demonstrate the capability of this design tool. The best three designs generated by the GA optimization are given in Table 1. All of the best designs have a maximum value for bolt diameter. The difference among them is in the horizontal locations of the bolts. For the joint with a three-row staggered pattern, the best three designs are given in Table 2. The maximum value of the evaluation function is reached for the design lay-up [25/50/25] and a bolt diameter of 8 mm. Details of the approach are described in a manuscript by Kradinov et al. (1998).

Table 1. The best designs for a three-fastener joint after GA strength optimization.

Parameters				Evaluation Function, F
Lay-Up	S_1 (mm)	S_2 (mm)	D (mm)	
[30/60/10]	16.0	15.0	8.0	20.72686
[30/60/10]	16.0	16.0	8.0	20.68473
[30/60/10]	15.0	16.0	8.0	20.57976

Table 2. The best designs for a three-row staggered joint after GA strength optimization.

Parameters			Evaluation Function, F
Lay-Up	S (mm)	D (mm)	
[25/50/25]	30.0	8.0	27.32952
[25/50/25]	30.0	6.0	26.46144
[25/50/25]	30.0	4.0	25.92354

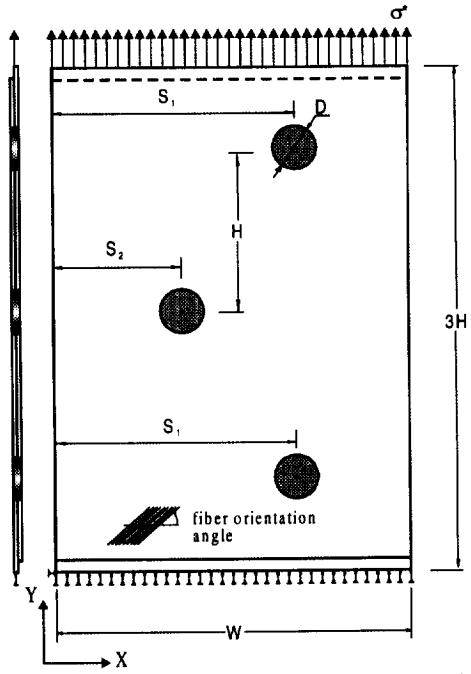

Figure 14. Geometric parameters of a three-fastener single-lap joint.

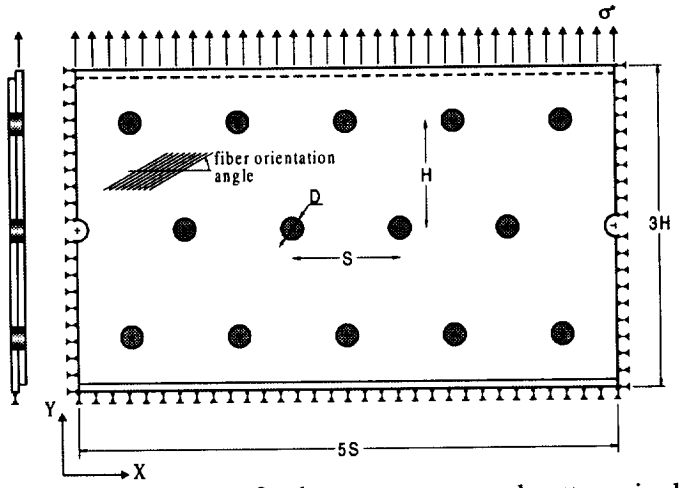

Figure 15. Geometric parameters of a three-row staggered-pattern single-lap joint.

Probabilistic and Deterministic Approach for Multi-Site Damage

We developed a probabilistic and deterministic approach to determine the reliability of aircraft structural components with multi-site damage. The major difference between this approach and those of others is that a three-parameter log-normal distribution of the residual time is constructed to determine the probability of failure as a function of residual life time.

This approach is based on the following assumptions: (1) Under cycling loading with constant amplitude, structural failure is comprised of crack initiation and propagation at critical locations. (2) Critical locations have individual fatigue-life and crack-growth characteristics. (3) A two-parameter and a three-parameter log-normal distribution represent fatigue life and crack growth, respectively. (4) Fatigue-life prediction prior to initial crack and cumulative damage is based on Miner's rule. (5) An elastic stress analysis with Neuber-type plasticity correction is used for fatigue-life prediction and crack growth for a specific number of cycling loadings. (6) Crack link-up criteria establish the residual life threshold until global failure occurs.

In order to demonstrate the fidelity of this approach, we considered a panel with three holes under cyclic loading. A typical stress field associated with randomly generated crack initiation sites and their growth is shown in Figure 16. The statistical log-normal distribution function, shown in Figure 17, was constructed by using a Monte-Carlo simulation in conjunction with the statistical models and parameters for crack initiation and growth. For comparison, a two-parameter distribution is also shown in this figure. It is apparent that inclusion of the threshold value influences the residual life estimation significantly in the range of 10^{-5} to 10^{-6}, which is representative of practical values. In order to render the computational effort more practical, a simplified approach was also developed for determination of the three parameters in the distribution function, shown in Figure 16. Though it provides acceptable correlation, further investigation is necessary for validation. A manuscript by describing the underlying concepts of this approach is being prepared and will be submitted for publication. The boundary collocation method for analysis of plane bolted joints was used in this work. The failure process was modeled as a stochastic chain of crack initiations, growth, linkups, and global failure.

Publications

The new methods developed under this grant have been disseminated in the form of journal publications and conference presentations as follows:

Barut, A. Madenci, E., Tessler, A., and Starnes, J. H., Jr., 1999, "A New Stiffened Shell Element for Geometrically Nonlinear Analysis of Composite Laminates," *Computers and Structures* (accepted).

Sergeev, B., Madenci, E., and Ambur, D. R., 1999, "Analysis of a Longeron Web with a Hole and an Arbitrarily Located Crack," *Theoretical and Applied Fracture Mechanics* (in-press).

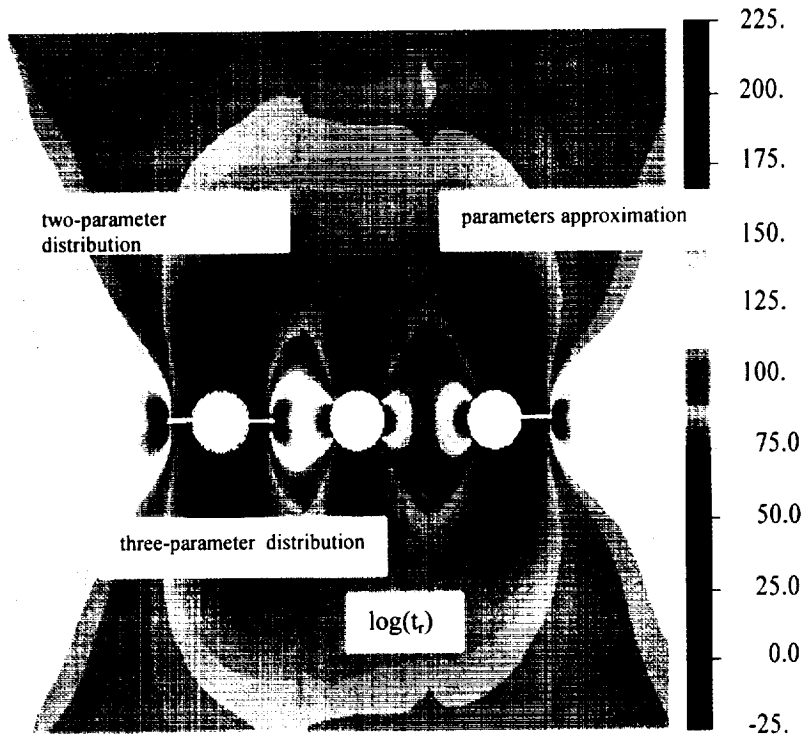

Figure 15. Typical stress distribution (σ_{yy}, MPa) in the loading direction in a panel with three fastener holes subjected to cycling loading.

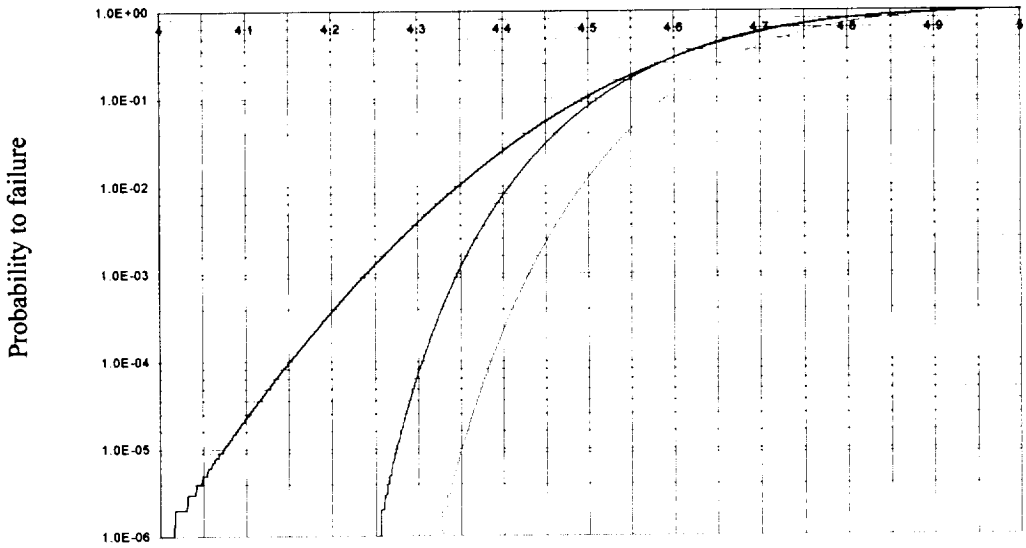

Figure 16. Probability of failure as a function of residual life.

Sergeev, B., Madenci, E., and Ambur, D. R., 1998, " Influence of Bolt Spacing and Degree of Laminate Anisotropy in Single-Lap Joints," NATO-ASI on Mechanics of Composite Materials and Structures, Trioa, Portugal (also accepted for publication in a special issue of *Computers and Structures*).

Kradinov, V., Madenci, E., Shkarayev, S., and Ambur, D. R., 1998, "Optimum Design for Single-Lap Bolted Composite Joints Using a Genetic Algorithm," *Theoretical and Applied Fracture Mechanics* (submitted).

Madenci, E., Barut, A., and Nemeth, M. P., 1998, " Coupled In-Plane and Bending Analysis of a Finite Geometry Nonsymmetric Laminate with an Elliptical Cutout by a Complex Variational Formulation," *ASME Journal of Applied Mechanics* (submitted).

References

Barut, A., Madenci, E., Tessler, A., and Starnes, J. H., Jr., 1998, "A New Stiffened Shell Element for geometrically Nonlinear Analysis of Composite Laminates," *Computers and Structures* (accepted)

Jiang, L. and Chernuka, M. W., 1995, "An Eccentrically Stiffened Shell Element Model with Geometrically Non-Linear Capability," Engineering Computations, Vol. 12, pp. 451-467.

Liao, C. L. and Reddy, J. N., 1989, " Continuum-Based Stiffened Composite Shell Element for Geometrically Nonlinear Analysis," AIAA journal, Vol. 27, pp. 95-101.

Kradinov, V., Madenci, E., Shkarayev, S., and Ambur, D. R., 1998, "Optimum Design for Single-Lap Bolted Joints Using a Genetic Algorithm," *Theoretical and Applied Fracture Mechaincs* (submitted)

Madenci, E., Barut, A., and Nemeth, M. P., 1998, "A Complex Potential-Variational Method for Stress Analysis of Unsymmetrically Laminated Plates with an Inclined Cutout," ASME *Journal of Applied Mechanics* (submitted).

Sergeev, B., Madenci, E., Ambur, D. R., 1998, "Influence of Bolt Spacing and Degree of Laminate Anisotropy in Single-Lap Joinst," NATO-ASI on Mechanics of Composite Materials and Structures, Trioa, Portugal.